The effect of selective deuteration on magnetization transfer in larger proteins

Ruth Pachter*, Cheryl H. Arrowsmith* and Oleg Jardetzky**

Stanford Magnetic Resonance Laboratory, Stanford University, Stanford, CA 94305-5055, U.S.A.

SUMMARY

The effects of selective deuteration on calculated NOESY intensities have been analyzed for the structure of the *E. coli trp* aporepressor, a 25 kDa protein. It is shown that selectively deuterated *trp* aporepressor proteins display larger calculated NOESY intensities than those for the same interproton distances in the natural abundance protein. The relatively larger magnetization transfer is demonstrated by a comparison of the NOE build-up curves for specific proton pairs, and for the calculated NOE intensities of short-range NOEs to backbone amide protons. This increase in intensity is especially pronounced for the NH^i-NH^{i+1} cross peaks in the α-helical regions, and particularly for amide protons of two sequential deuterated residues. The effect is shown to be further intensified for longer mixing times. It is also shown that in all cases, each amide proton exhibits stronger NOEs to its own side chain, with an enhanced effect for deuterated derivatives. This theoretical analysis demonstrates that an evaluation of the relative NOE intensities for different selectively deuterated analogs may be an important tool in assigning NMR spectra of large proteins. These results also serve as a guide for the interpretation of NOEs in terms of distances for structure calculations based on data using selectively deuterated proteins.

INTRODUCTION

Although ^{1}H-^{1}H nuclear Overhauser enhancement spectroscopy (NOESY) is well established as a powerful technique for the determination of the spatial proximity of protons in small proteins (Wüthrich, 1986), a straightforward extension of this methodology to structural studies of large biomolecules is not as yet generally applicable. This limitation is due both to line broadening re-

sulting from the short relaxation times for large proteins and to the large degree of overlap in spectra of large proteins. In order to overcome these difficulties, methods involving isotopic labeling are necessary for the assignment of NMR spectra of proteins with molecular weights above 10–15 kDa (for reviews see Stockman and Markley, 1989; Fesik and Zuiderweg, 1990; LeMaster, 1990; Clore and Gronenborn, 1991). Uniform labeling with ^{13}C and ^{15}N allows one to overcome the overlap problem by extending the dimensionality of the NMR experiment using the heteronuclear resonance frequencies and also circumvents the limitations of short proton T_2s by making use of the relatively large heteronuclear one-bond couplings (Bax et al., 1990a,b; Ikura et al., 1990; Kay et al, 1990a,b; Clore et al., 1991). Alternative isotope-assisted strategies involve deuterium labeling. If a relatively high level of deuterium is incorporated into the protein, each of the remaining protons in the structure is surrounded by fewer other protons, and will have fewer pathways for cross relaxation, resulting in longer relaxation times, and consequently narrower linewidths and improved resolution.

Random fractional deuteration (LeMaster and Richards, 1988) greatly reduces the overall linewidths of proton resonances, however, the spectral overlap in a 2D NOESY spectrum is still significant, especially in proteins with molecular weights > 10 kDa. Selective deuteration (Markley et al., 1968) results in better alleviation of the overlap problem, although it does not do as well as 3D and 4D heteronuclear methods. In selective deuteration, however, proton relaxation times are not as drastically reduced as for random fractional deuteration due to efficient cross relaxation between protons within each protonated side chain. Therefore selective deuteration has enjoyed increasing popularity in recent years for the study of larger proteins: transcription factor 1 from *Bacillus subtilis* (23 kDa, Reisman et al., 1991), *E. coli trp*-repressor (25 kDa, Arrowsmith et al., 1990a) and peptide antibody Fab' complex (56 kDa, Tsang et al., 1990). In each of these studies as well as one for perdeuterated staphylococcal nuclease (18 kDa, Torchia et al., 1988) dramatic effects on NOE intensities have been observed due to deuteration, especially for NOEs involving NH protons.

In order to use NOE information from deuterium-assisted protein spectroscopy, a detailed theoretical investigation of the effect of deuteration on NOESY intensities in large proteins is required, especially if the results are to be used for distance constraints in structure calculations. The results of such a theoretical evaluation can help in the interpretation of future NMR studies of large proteins involving selective deuterium labeling. We have recently determined low-resolution NMR structures of *E. coli trp*-repressor and aporepressor (25 kDa) based on a minimum set of interresidue NOEs gathered from a series of selectively deuterated proteins (Arrowsmith et al., 1991). Before a refinement to higher resolution is attempted, a better understanding of the effects of selective deuteration on NOE intensities is necessary. Magnetization transfer by cross relaxation in a two-dimensional NOE experiment can be simulated by solving the generalized Bloch equations (Madrid and Jardetzky, 1988; Summers et al., 1990) for any given system of protons. However, problems may arise in the application of these computations to solution structures of large molecules. Specifically, NOE intensities calculated by using the Bloch equations are significantly affected by small distance changes (Madrid and Jardetzky, 1988). In addition, correlation time variations within different regions of the protein, which may contribute to the NOESY intensity (Madrid et al., 1989), are not taken into account. Indeed, the first successful detailed quantitative comparison of experimental and back-calculated spectra was recently shown to be possible only by using an iterative approach with comprehensive data-fitting procedures for an 18-

residue peptide (Summers et al., 1990). In the present application, the analysis of computational results is concerned only with the *relative* NOE intensities between different deuterated analogs and the natural abundance repressor molecule. No absolute intensity predictions are attempted, and the theoretical results are compared to experimental data only in qualitative terms. Also, since the crystallographic structure is more precise for the purpose of addition of hydrogens to the heavy-atom framework, this comparative theoretical study is based on an X-ray structure of the protein.

METHOD

Theory

Cross relaxation of the longitudinal magnetization components in a two-dimensional ^1H-^1H NOE experiment proceeds with time according to the well-known Bloch–Solomon equation (Solomon, 1955):

$$\dot{M} = -\Gamma M \tag{1}$$

where M describes the magnetization deviations from those at thermal equilibrium (M(0)) for all spins i (i = 1,...N), and Γ represents the (N × N) matrix of relaxation rates. The elements of the matrix Γ, namely, the intrinsic spin lattice relaxation rates ρ_i and the cross-relaxation rate constants σ_{ij} for two interacting spins $\{i \neq j\}$, are given by:

$$\rho_i = \kappa \, \Sigma_i \, (1/r_{ij}^6) \, (6J_2 + 3J_1 + J_0)$$
$$\sigma_{ij} = \kappa \, (1/r_{ij}^6) \, (6J_2 - J_0) \tag{2}$$

where the summation is over all spins, and $J_n(\omega) = \{\tau_c/(1 + n^2\omega_{ij}^2\tau_c^2)\}$ are the spectral density functions. These functions depend on the ω_{ij} Larmor frequencies of the interacting spins, and the rotational correlation time τ_c of the protein molecule (in ns). The r_{ij} interproton distances are in Å, and $\kappa = 0.1\gamma_H^4 \, (h/2\pi)^2 \, (= 56.83 \, Å^6ns^{-2}$, where γ is the hydrogen gyromagnetic ratio and h is Planck's constant).

Equation (1) can be rewritten, so that for any spin i:

$$dM_i/dt = -\rho_i \, (M_i - M_i(0)) - \Sigma\sigma_{ij} \, (M_j - M_j(0)), \, i \neq j \tag{3}$$

solved formally for a mixing time t_m by (Macura and Ernst, 1980):

$$M_i(t_m) = \Sigma_k \, a_{ik}(t_m) \, M_k(0) \tag{4}$$

where the $a_{ik}(t_m) = \{e^{-\Gamma t_m}\}_{ik}$ values are proportional to NOE intensities. For specific initial conditions, and a given geometry of the molecule (r_{ij} distance matrix) and its correlation time τ_c, this set of N simultaneous equations can be solved either numerically, or by a diagonalization of the relaxation matrix. The two techniques are equivalent if the integration step size Δt is suitably chosen (Madrid and Jardetzky, 1988; Banks et al., 1989; Forster, 1991).

Computational details

Theoretical NOESY calculations were performed by using the Euler method for a numerical integration of the generalized Bloch equations (Jardetzky et al., 1986; Madrid and Jardetzky, 1988). The a_{ik} matrix elements of Eq. (4) were obtained by selecting as initial conditions $M_k(0) = 0$ for $k \neq 1$, and $M_1(0) = 1$. The integration step size Δt was chosen so that it is always smaller than the minimal relaxation time in the protein, and also small enough for a meaningful integration. In addition, for a specific upper limit on the mixing time, e.g. 200 ms, Δt is to be inversely proportional to the number of cycles for the integration. Integration of the Bloch equations was used, since it proved to be faster than the diagonalization method (Banks et al., 1989), and in addition, only one calculation is necessary for an evaluation of the intensity dependence on various mixing times.

Internuclear proton–proton distances for the NOESY simulations were generated from the coordinates of the X-ray structure of the *trp* aporepressor (Zhang et al., 1987). *trp* aporepressor is a symmetric dimer with 107 amino acids per monomer, and composed almost entirely of α-helix and short surface turns. Hydrogen atoms with standard bond lengths and angles were added to the atomic Cartesian coordinates (Jarvis et al., 1986) derived from the crystallographic data in the Brookhaven Protein Data Bank. An interproton distance matrix could then be obtained, where distances larger than 6 Å were neglected (Summers et al., 1990). Methyl groups were considered to be single nuclei, centered at the mean atomic position of the three protons, with spins I of 3/2.

TABLE 1

SELECTIVELY DEUTERATED[a] *trp*-APOREPRESSOR ANALOGS

Amino acids		Analogs[b]		
		HLW	GMAPS	GRIFSTV
Ala	(10)	-		
Arg	(9)	E	E	
Asx	(9)	E		
Gly	(5)	E		
Glx	(19)			-
His	(2)		E	E
Ile	(3)	E	E	-
Leu	(19)		E	E
Lys	(4)	E	E	E
Met	(3)	E		E
Phe	(1)	E	E	
Pro	(5)	E	-	E
Ser	(6)			
Thr	(4)	E	E	
Trp	(2)			
Tyr	(2)	E	E	E
Val	(5)	E	E	-

[a] E = Experimentally less than 20% of the hydrogens of these residues are protonated per monomer, and thus these residues are eliminated from the distance matrix used for the Bloch calculation. The number of each amino acid type per monomer is indicated in parentheses.

[b] Names of analogs correspond roughly to the one-letter amino acid code of protonated residues.

A uniform overall tumbling time τ_c of the protein (~ 8 ns) was determined from the molecular weight by the Stokes–Einstein relationship, $\tau_c = \{\eta V/kT\}$, where V is the hydrated molecular volume, η the solvent viscosity, T the temperature, and k is the Boltzmann constant. The spectrometer frequency ($\omega_0/2\pi$) equals 500 MHz, and the spectra were simulated at a temperature of 45°C, at mixing times of 50, 100, 160, and 200 ms. The threshold for a calculated NOE observation was set to 0.01 (i.e., 1% relative to the intensity of the diagonal peak at time $t_m = 0$ ms). This NOE intensity unit (%) is used in the subsequent discussion. Three selectively deuterated analogs (summarized in Table 1), which were studied experimentally (Arrowsmith et al., 1990a) were simulated by an elimination of the appropriate hydrogen–hydrogen connectivities from the distance matrix. Thus, the resulting simulations involved Bloch equation calculations of 679, 448, 386, and 468 coupled equations for the protonated protein, and the HLW, GMAPS, and GRIFSTV deuterated analogs (from Arrowsmith et al., 1990a), respectively. All calculations were performed on a Cray X-MP supercomputer.

RESULTS AND DISCUSSION

NOE build-up

In general, the deuterated derivatives of the *trp* aporepressor display larger calculated NOESY intensities than those for the same interproton distances in the natural abundance protein. This relatively larger magnetization transfer is demonstrated, for example, by a comparison of the NOE build-up curves for the pair of protons $\{CH_3$ Ala^{29}-H6 Trp$^{99}\}$ in the protonated repressor
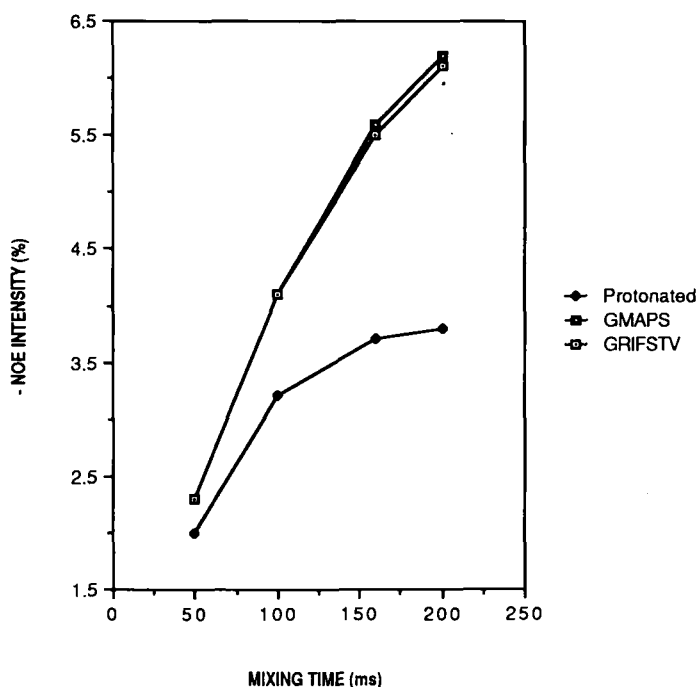

Fig. 1. The time dependence of the calculated NOE intensity between the methyl protons of Ala^{29} and H6 of Trp^{99} in the natural abundance repressor, and the selectively deuterated analogs GMAPS and GRIFSTV.

and both the GMAPS and GRIFSTV deuterated derivatives. It is shown in Fig. 1 that the maximal intensity in the natural abundance protein is about 3.5%, while in the deuterated proteins it is larger than 6%. This is undoubtedly a consequence of fewer pathways for magnetization transfer in the deuterated proteins resulting in less overall spin diffusion. This is also demonstrated by the data in Table 2 which shows larger average values for various types of sequential NOEs (those involving short-range NOEs to backbone amide protons) in selectively deuterated proteins. Similar results were also recently observed for a 23 kDa protein by Reisman et al. (1991). Even more interesting than the overall greater intensity is the large and predictable variation in intensity of sequential NOEs with the deuteration pattern of the protein. Sequential NOEs define the secondary structure of proteins, and it is therefore important to understand the factors affecting their intensities if they are to be interpreted correctly.

NH^i-NH^{i+1} NOEs

Significant improvement in NOE intensities has been observed between NH protons in helical regions of an 18 kDa perdeuterated protein (Torchia et al., 1988) and a selectively deuterated peptide in a 56 kDa complex (Tsang et al., 1990). We also observed increased NH-NH intensities as well as large variations in intensity between different deuterated analogs corresponding to the deuteration pattern (Arrowsmith et al., 1990a,b). This phenomenon results from competitive pathways for magnetization transfer from any amide proton (NH^i) to either the NH of the neighboring residue (NH^{i+1}, NH^{i-1}), or to its α-proton ($C_\alpha H^i$). In an α-helix NH^{i+1}, NH^{i-1} and $C_\alpha H^i$ are at comparable distances (< 3 Å) from NH^i. If residue i is protonated, magnetization is transferred from NH^i to $C_\alpha H^i$ and then further down side chain i. However, if residue i is deuterated, this pathway is eliminated, and most of the amide proton magnetization is transferred to the NH of the neighboring residues. Thus, the magnetization transferred from amide protons of protonated residues is partially diffused, and consequently, the intensities of NH^i-NH^{i+1} NOEs of deuterated residues will be larger. Figure 2 shows the calculated NH^i-NH^{i+1} NOE intensities for the three different selectively deuterated proteins. The left-hand panel shows the NOE intensity (relative to natural abundance repressor) vs. residue number. All intensities in the deuterated protein are greater than those at natural abundance and the variation in intensity reflects the pattern of deuteration. These calculated intensities correspond *qualitatively* to those observed experimentally. For example, the right-hand panel of Fig. 2 shows the portion of the NOESY spectrum containing cross peaks between NHs 53–54, 54–55, 38–39 and 39–40. The corresponding points in the calculated data are circled. The NOEs involving the NH of Arg[54] are strongest in HLW where all

TABLE 2
AVERAGE CALCULATED NOE INTENSITIES[a] (AND THEIR NUMBER FOR ONE MONOMER) IN THE NATURAL ABUNDANCE, AND TWO SELECTIVELY DEUTERATED ANALOGS OF THE *trp*-REPRESSOR

	Protonated repressor	GMAPS	GRIFSTV
$NH^i - \{C_{\alpha,\beta,\gamma,}\}H^i$	3.0 (478)	4.8 (204)	3.9 (310)
$NH^i - \{C_{\alpha,\beta,\gamma,}\}H^{i-1}$	2.0 (324)	3.1 (200)	2.4 (247)
$NH^i - C_\alpha H^{i-3}$	1.5 (52)	1.6 (27)	1.6 (39)
$NH^i - NH^{i+1}$	2.3 (85)	3.6 (88)	3.6 (87)

[a] The intensities (-NOE) are given in %, and were computed by a Bloch equation simulation at a mixing time of 200 ms.

VARIATION OF NH-NH NOE INTENSITIES WITH DEUTERATION
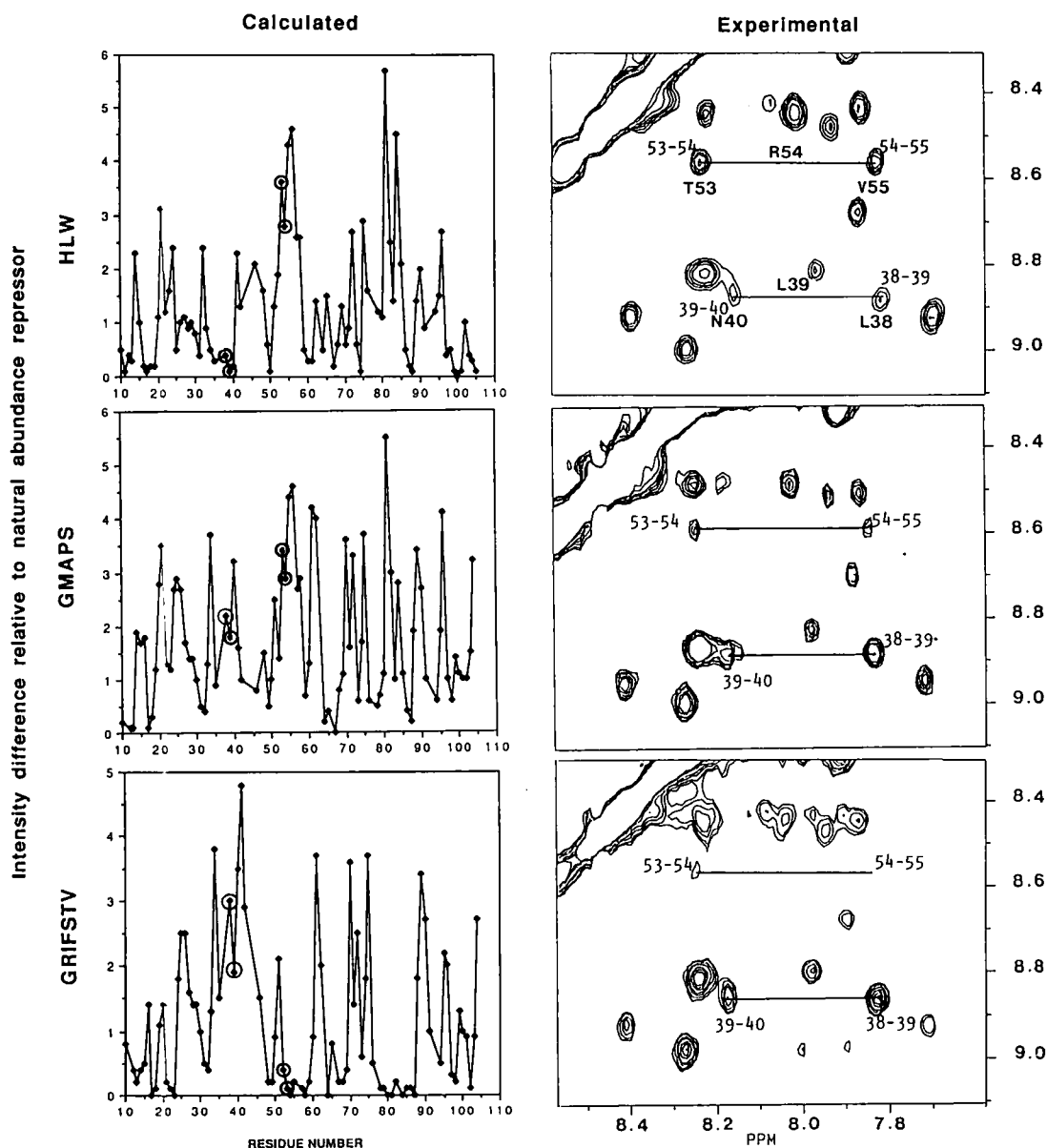
Calculated

Experimental

Fig. 2. Comparison of experimental and calculated NOE intensities in selectively deuterated *trp*-repressor analogs. Left: selected calculated NOE intensities relative to those in the protonated repressor. NOEs between NHs 53–54, 54–55, 38–39 and 39–40 are in circles. Right: the corresponding experimental NOEs (labeled in top spectrum). NMR spectra and deuterated proteins were prepared as described in Arrowsmith et al. (1990a,b).

three residues (T53, R54 and V55) are deuterated and weakest in GRIFSTV where these residues are protonated. A similar trend is seen for the NOEs involving the NH of Leu[39]. A more quantitative comparison is not warranted at this time due to the incomplete deuteration of some residues

190

in the experimental samples (see Arrowsmith et al., 1990a,b) and the problems associated with differential correlation times since *trp*-repressor is known to have separate rigid and flexible regions (Arrowsmith et al., 1991; Czaplicki et al., 1991). A similar theoretical prediction of NH-NH NOE intensities was reported by Tsang et al. (1990) for two pairs of NH protons in a helical selectively deuterated peptide bound to an FAB' fragment.

The calculations also demonstrate that this effect is intensified for a longer mixing time, as pointed out by Torchia et al. (1988). Figure 3 shows the results of simulations for GMAPS at mixing times of 100 and 200 ms. The intensities of the NOEs involving deuterated residues get larger at the longer mixing time, while those for protonated residues change very little. All of these results demonstrate that the intensities of the NH^i-NH^{i+1} cross peaks in NOESY spectra of different deuterated analogs are highly dependent on the deuteration pattern. This variation in intensity can be a valuable aid in assigning the ^1H NMR spectrum of selectively deuterated proteins (Arrowsmith et al., 1990a).

NH^{i-} side chain or $C_\alpha H^{i-3}$ NOEs

In assignment procedures for small proteins based on the sequential assignment method (Gibbons et al., 1975; Wüthrich, 1986) NOEs from amide protons can be identified as inter- or intraresidue NOEs based on direct or relayed scalar couplings from the amide proton to its own side-chain protons. In larger proteins information based on proton–proton scalar coupling is often absent due to broad linewidths. Therefore alternative information is needed in order to distinguish between inter- and intraresidue NOEs from amide protons. In light of the large but predictable variation of NH-NH NOE intensity caused by deuteration, it is instructive to examine the effect of deuteration on NOEs from NH to side-chain protons. In the NOE-based assignment procedures recently described for the *trp*-repressor (Arrowsmith et al., 1990a), we observed that NOEs from amide protons to adjacent side chains, i.e. $NH^i - \{C_{\alpha,\beta,\gamma,...}\}H^{i-1}$ or $NH^i - C_\alpha H^{i-3}$, are of weaker intensity than the corresponding NOEs within the same side chain, namely $NH^i -$
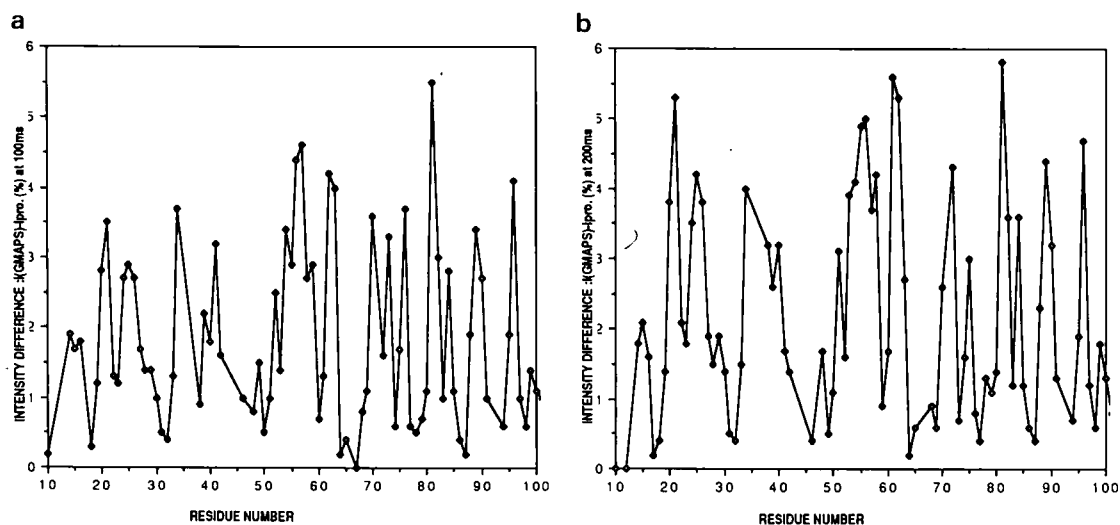

Fig. 3. (a) Calculated intensity differences of deuterated residues at 100 ms and (b) at 200 ms, between the natural abundance *trp*-repressor and the selectively deuterated analog (GMAPS) as a function of residue number.

$\{C_{\alpha,\beta,\gamma...}\}H^i$. This phenomenon is reproduced in the present theoretical data reported in Table 2. As expected from the distance, the average NOE intensities in the natural abundance protonated repressor, as well as for the two deuterated analogs, reflect the fact that in all cases each amide proton exhibits the stronger NOEs to its own side chain. Also, the effect is enhanced for the deuterated derivatives, i.e. this difference in intensity is about 40% for the deuterated analogs, as compared to 30% in the natural abundance repressor. A specific example is listed in Table 3. Obviously, the actual number of NH^i to other $\{C_{\alpha,\beta,\gamma...}\}H$ protons is significantly lower in the deuterated analogs, thereby improving the problem of crowding in NOESY spectra. From Table 2 it is clear that selective deuteration has the greatest effect on the sequential $NH^i - NH^{i+1}$ NOEs and intraresidue NOEs, while having very little effect on the helical $NH^i - C_\alpha H^{i-3}$ NOEs. Nevertheless, several $NH^i - C_\alpha H^{i-3}$ connectivities not present in the calculated spectrum of the protonated protein do appear in those of the deuterated analogs, for example, residues i = 20, 34, 52, 62, 67, 96 in GMAPS, and residues i = 20, 34, 58, 59, 60, 100 in GRIFSTV. Except for residues 34 and 67, these are all in α-helical regions of the protein. The absence of the $NH^i - C_\alpha H^{i-3}$ cross peak in the natural abundance repressor is due to spin diffusion which reduces the intensity of these cross peaks. It does *not* indicate that the two protons involved are not close enough to exchange magnetization and generate an NOE cross peak.

Cross-peak intensity–distance relationship

The relationship between the calculated NOESY cross-peak intensities (I) and the corresponding internuclear distances in the natural abundance *trp*-repressor, and all of its· deuterated analogs, was evaluated. The results are displayed for the protonated repressor and the HLW analog (Figs. 4a and b, respectively). Amide protons were not included in these plots since we

TABLE 3

CALCULATED NOE INTENSITIES[a] IN THE GMAPS DEUTERATED DERIVATIVE OF THE *trp*-APOREPRESSOR

$NH^i - \{C_{\alpha,\beta,\gamma}\}H^i$			$NH^i - \{C_{\alpha,\beta,\gamma}\}H^{i-1}$		
i = Glu[19]	i = Glu[19]		i = Glu[19]	i − 1 = Gln[17]	
HN	H1B	4.3	HN	H1B	2.7
	H2B	4.7		H2B	2.8
	HA	3.8		HA	1.7
	H1G	4.3		H1G	1.9
	H2G	4.2		H2G	1.9
i = Trp[19]	i = Trp[19]		i = Trp[19]	i − 1 = Glu[18]	
HN	H1B	6.8	HN	H1B	2.8
	H2B	6.9		H2B	3.2
	HA	4.5		HA	1.9
	HD1	3.5		H1G	1.8
	HE3	1.8		H2G	1.7

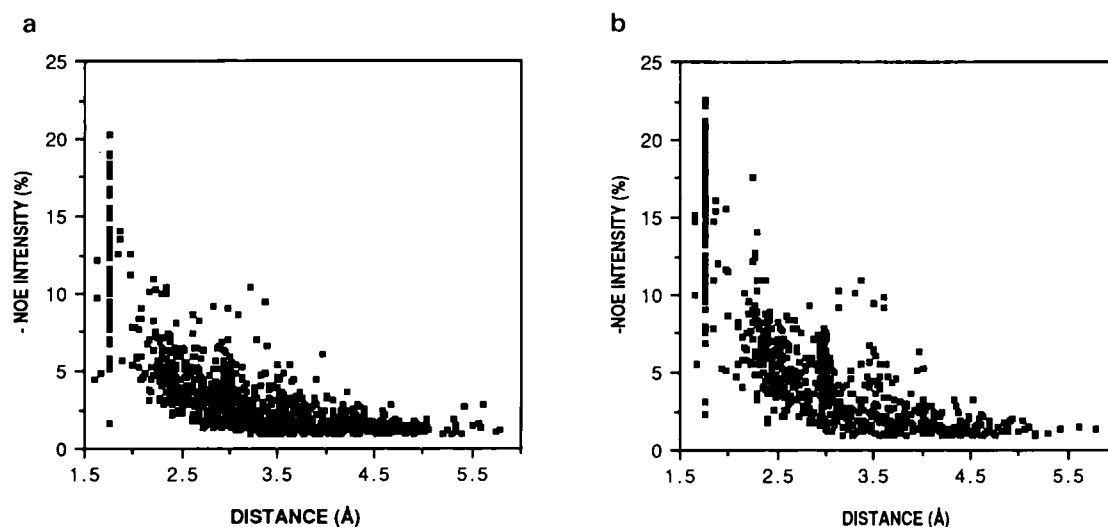[a] See footnote [a] of Table 2.

a

b

Fig. 4. (a) NOE intensity vs. distance relationship for selected pairs of protons (see text) of protonated natural abundance *trp*-repressor, and (b) its deuterated analog HLW. The cross-peak intensities were recorded at a mixing time of 100 ms.

have already shown their intensity can change depending on the deuteration pattern. Also, the CH_3 methyl group protons produce cross peaks of higher intensity because their effective spin is three times higher (3/2), and were therefore also excluded from the correlation. Although least-squares correlations of I vs. $(1/r^6)$ yield somewhat larger correlation coefficients for the HLW and GMAPS derivatives ($r = 0.83$, and $r = 0.81$, respectively), as compared to that for the protonated protein ($r = 0.78$), the accuracy of distance prediction from the NOESY cross-peak intensities assuming such a two-spin approximation is, as expected, relatively low for a protein of this molecular weight. Thus, for nonamide proton NOEs it appears that the rough classification of strong, medium and weak NOEs into three broad distance ranges is appropriate for selectively deuterated proteins.

In conclusion, the results presented in this study show that selective deuteration of a protein has a substantial influence on the intensity of the NOE cross peaks between the remaining protons. This forms a basis for the interpretation of NOE intensities from deuterated proteins in terms of distances. For a specific structure, the NOE intensity can vary up to 6% of the initial diagonal peak intensity, depending on the deuteration pattern. This is the result of competitive pathways for magnetization transfer, some of which are eliminated by deuteration. This increase in intensity is especially pronounced for the NH^i-NH^{i+1} cross peaks in the α-helical regions of the *trp*-repressor, and particularly for amide protons of two sequential deuterated residues. The effect is shown to be further intensified for longer mixing times. In addition, Bloch equation simulations of the *trp* aporepressor NOESY spectra show that in all cases each amide proton exhibits stronger NOEs to its own side chain, with an enhanced effect for deuterated derivatives. Selective deuteration does not appear to affect the relatively imprecise relationship between interproton distance and NOE intensity for nonamide proton NOEs. Thus, NOEs involving amide protons must be interpreted more conservatively (in terms of distance) to account for the effects of deuterations, while non-amide NOEs can apparently be interpreted in a manner similar to those for natural abundance

proteins of equivalent molecular weight. Finally, the theoretical analysis presented in this paper demonstrates that the relative NOE intensities for different selectively deuterated analogs can be an important tool in assigning NMR spectra of large proteins. In fact, we have assigned greater than 80% of the resonances of the *trp*-repressor dimer (25 kDa) using an NOE-based strategy and relying on these *qualitative* effects of selective deuteration. The data presented here also indicate that some level of deuteration may be required in proteins larger than 25 kDa if the NOE intensities are going to be large enough to be observed experimentally (see also Tsang et al., 1990). Thus, in the future, selective deuteration (or random fractional deuteration, LeMaster and Richards, 1988) combined with the powerful multidimensional heteronuclear methods (Bax et al., 1990a,b; Ikura et al., 1990, 1991; Kay et al., 1990a,b) should extend the useful application of NMR to much larger proteins or protein complexes.

ACKNOWLEDGEMENTS

REFERENCES

Arrowsmith, C.H., Czaplicki, J., Iyer, S.B. and Jardetzky, O. (1991) *J. Am. Chem. Soc.*, **113**, 4020 4022.

Arrowsmith, C., Pachter, R., Altman, R. and Jardetzky, O. (1991) *Eur. J. Biochem.*, **202**, 53 66.

Arrowsmith, C.H., Pachter, R., Altman, R.B., Iyer, S.B. and Jardetzky, O. (1990a) *Biochemistry*, **29**, 6332 6341.

Arrowsmith, C.H., Treat-Clemons, L., Szilágyi, L., Pachter, R. and Jardetzky, O. (1990b) In *Die Makromolekulare Chemie, Macromolecular Symposia* (Proceedings of the 9th Colloque Ampere, *Magnetic Resonance in Polymers*, Prague, Czech.), **34**, 33 46.

Banks, K.M., Hare, D.R. and Reid, B.R. (1989) *Biochemistry*, **28**, 6996 7010.

Bax, A., Clore, G.M., Driscoll, P.C., Gronenborn, A.M., Ikura, M. and Kay, L.E. (1990a) *J. Magn. Reson.*, **87**, 620 627.

Bax, A., Clore, G.M. and Gronenborn, A.M. (1990b) *J. Magn. Reson.*, **88**, 425 431.

Clore, G.M. and Gronenborn, A.M. (1991) *Science*, **252**, 1390 1399.

Clore, G.M., Kay, L.E., Bax, A. and Gronenborn, A.M. (1991) *Biochemistry*, **30**, 12 18.

Czaplicki, J., Arrowsmith, C. and Jardetzky, O. (1991) *J. Biomol. NMR*, **1**, 349 361.

Fesik, S.W. and Zuiderweg, E.R.P. (1990) *Quart. Rev. Biophys.*, **23**, 97 132.

Forster, J.M. (1991) *J. Comp. Chem.*, **12**, 292 300.

Gibbons, W.A., Crepaux, D., Delayre, J., Dunand, J.J. Hajdukovic, G. and Wyssbrod, H.R. (1975) In *Peptides: Chemistry, Structure and Biology* (Eds. Walter, R. and Meienhofer, J.) Ann Arbor Science, Ann Arbor, pp. 127 137.

Ikura, M., Kay, L.E. and Bax, A. (1990) *Biochemistry*, **29**, 4659 4667.

Ikura, M., Kay, L.E., Krinks, M. and Bax, A. (1991) *Biochemistry*, **30**, 5498 5504.

Jardetzky, O., Lane, A., Lefèvre, J.-F., Lichtarge, O., Hayes-Roth, B., Altman, R. and Buchanan, B. (1986) In *Proceedings XXIII Congress Ampere on Magnetic Resonance* (Eds. Maraviglia, B., De Luca, F. and Campanella, R.) Rome, Italy, pp. 46 69.

Jarvis, L., Huang, C., Ferrin, T. and Langridge, R. (1986) *UCSF MIDAS Molecular Interactive Display and Simulation*, University of California, San Francisco. (The ADDHYDROGEN program of the MIDAS package was used.)

Kay, L.E., Ikura, M. and Bax, A. (1990a) *J. Am. Chem. Soc.*, **112**, 888 889.

Kay, L.E., Ikura, M., Tschudin, R. and Bax, A. (1990b) *J. Magn. Reson.*, **89**, 496 514.

LeMaster, D.M. and Richards, F.M. (1988) *Biochemistry*, **27**, 142 150.

LeMaster, D.M. (1990) *Quart. Rev. Biophys.*, **23**, 133 174.

Macura, S. and Ernst, R.R. (1980) *Mol. Phys.*, **41**, 95 117.

Madrid, M. and Jardetzky, O. (1988) *Biochim. Biophys. Acta*, **953**, 61 69.

Madrid, M., Mace, J.E. and Jardetzky, O. (1989) *J. Magn. Reson.*, **83**, 267 278.

Reisman, J., Jariel-Encontre, I., Hsu, V.L., Parello, H., Geiduschek, E.P. and Kearns, D.R. (1991) *J. Am. Chem. Soc.*, **113**, 2787-2789.

Solomon, I. (1995) *Phys. Rev.*, **99**, 559.

Stockman, B.J. and Markley, J.L. (1989) In *Protein Structure and Engineering* (Ed., Jardetzky, O.) Plenum Press, N.Y., pp. 155-192.

Summers, M.F., South, T.L., Kim, B. and Hare, D.R. (1990) *Biochemistry*, **29**, 329-340.

Torchia, D.A., Sparks, S.W. and Bax, A. (1988) *J. Am. Chem. Soc.*, **110**, 2320-2321.

Tsang, P., Wright, P.E. and Rance, M. (1990) *J. Am. Chem. Soc.*, **112**, 8183-8185.

Wüthrich, K. (1986) *NMR of Proteins and Nucleic Acids*, Wiley, New York.

Zhang, R.-G., Joachimiak, A., Lawson, C.L., Schevitz, R.W., Otwinowski, Z. and Sigler, P.B. (1987) *Nature*, **327**, 591-597.